Iranian Journal of Geophysics, 2021, Page 41 – 65 (Research)
DOI: 10.30499/ijg.2020.107329

Presenting an integrated strategy for porosity mapping in a genetic-based seismic inversion framework in a heterogeneous reservoir

Amin Shahbazi[1], Mehrdad Soleimani Monfared[2*], Vinesh Thiruchelvam[3] and Thang Ka Fei[4]

[1] Assistant Professor, Faculty of Engineering, Asia Pacific University of Technology & Innovation (APU), Kuala Lumpur, Malaysia
[2] Associate professor, Faculty of Mining, petroleum and Geophysics, Shahrood University of technology, Shahrood, Iran
[3] Professor, Faculty of Engineering, Asia Pacific University of Technology & Innovation (APU), Kuala Lumpur, Malaysia
[4] Associate Professor, Faculty of Engineering, Asia Pacific University of Technology & Innovation (APU), Kuala Lumpur, Malaysia

(Received: 15 March 2020, Accepted: 6 July 2020)

Abstract

Seismic reservoir characterization is a state-of-the-art procedure in using various sources of data. Generally, seismic data, due to their low resolution, are randomly used in the final steps of reservoir characterization. However, extensive coverage of 3D seismic data, compared to well data, makes it possible to be applicable for the distribution of characters through the whole reservoir. In this regard, seismic data should be inverted to illustrate the desired characters throughout the media. Conventionally, seismic inversion uses well logs that have defects in its derivation steps, such as wavelet extraction and its propagation through media. The proposed strategy to resolve such deficiencies is the genetic inversion. However, genetic inversion has its own deficiency in accuracy. In this study, we propose an integrated strategy for using various sources of data in an iterative manner for resolving this obstacle. The proposed strategy uses a combined related attribute to evaluate initial acoustic impedance inverted model by genetic inversion. The model then would be updated to satisfy well data. The proposed strategy was applied to a heterogeneous reservoir from the southwest of Iran. Three seismic attributes were integrated to produce a unique attribute for initial model evaluation. The final model was then evaluated by well data. Results were also compared with the conventional method of seismic inversion. The result of the proposed strategy in the genetic inversion depicted improvement in the final acoustic impedance and the porosity distribution model.

Keywords: Seismic reservoir characterization, Genetic inversion, Seismic attributes, Porosity distribution.

*Corresponding author: msoleimani@shahroodut.ac.ir

1 Introduction

Accurate representation of the subsurface geological structure and the rock properties model is an essential step in the sequence of reservoir characterization (Al-Bulushi et al. 2012). Various advanced methods are available to derive precise model of reservoir characteristics and provide information of reservoir properties in different scales (Chen and Durlofsky 2006). Seismic reservoir characterization in heterogeneous media is essential to resolve some of the ambiguities in petroleum field management. Previous studies have shown that the homogeneity of the porous media has the highest influence on production (namely 40%), while its effectiveness vanishes in heterogeneous media to 37% (Balouchi et al. 2013; Nozohour-leilabady and Fazelabdolabad 2015). Thus, an optimum practical approach consists of incorporating the impact of the reservoir heterogeneity in modeling reservoir characters (Benisch et al. 2015). Herewith, accurate modelling of reservoir properties, such as porosity and permeability, is essential. However, obtaining accurate and precise relationship between seismic parameters, which are the main sources of information in seismic reservoir characterization, is a challenging task, specifically in a heterogeneous reservoir even with simple structures (Ahmadi et al. 2015; Daraei et al. 2017). Various studies have shown that the distribution of reservoir characteristics, like porosity and permeability, depends on the rock properties of the reservoir, which could be extracted from seismic attributes (Maffucci et al. 2015, Soleimani 2017a). Hence, several studies have been performed to use seismic attributes in various strategies for seismic reservoir characterization. However, a seismic attribute by itself is not a reliable source of information. Therefore, it was proposed to combine various seismic attributes for seismic reservoir characterization (Noorbakhsh et al. 2014; Oyeyemi et al. 2019). This implies performing literature review on the selection of appropriate attributes for desired reservoir characteristics and, subsequently, an appropriate strategy for integration of selected attributes, to obtain a unique reliable model (Soleimani 2017b). However, an individual seismic attribute by itself could not be used directly for extraction of reservoir characters, but it should be used as an intermediate product or for evaluation of intermediate products, such as the acoustic impedance (Abdel-Rasoul et al. 2014). Mostly, selected attributes or any integrated attribute would be used for evaluation of the seismic inversion result. Since the acoustic impedance model conventionally is obtained by other sources of information, like sonic and density logs, evaluating its result with seismic attributes is not rationally acceptable (Ahmadi et al. 2015). In this study, we introduce a procedure for obtaining inversion result in such a way that could be evaluated by a combined single attribute result. The proposed strategy then would be applied on selected petroleum field in the southwest of Iran, with two reservoir target formations.

2 The proposed strategy for genetic inversion

The main components of a general workflow in seismic inversion for reservoir characterization consist of solving local auxiliary problems for target formation on the seismic cube (Iliev and Rybak 2008; Guerriero et al. 2012). The proposed strategy aims to resolve some of the ambiguities in the procedure of seismic inversion, required for further reservoir characterization. Obviously, result of the inversion procedure depends on the quality and accuracy of the results from the interpretation step, which also relates to precision in signal processing

procedure (Vatandoust and Farzipour Saein 2019). Figure 1 shows a simplified graphical flowchart of the proposed strategy, which would be applied on data from petroleum field under investigation. As an assumption, it was assumed that the processing procedure was applied adequately on data, which makes it appropriate for further interpretation. The whole procedure could be separated in three steps, the interpretation step, the inversion and attributes analysis step and finally the rock properties analysis step, which is also known as primary or initial seismic reservoir characterization. The interpretation step was divided into two separate parts as the seismic structural interpretation and the time – depth conversion (TDC) steps, using velocity analysis. The interpretation procedure performed on data consists of well data analysis, generation of synthetic seismogram for all the wells, (required for primary inversion) followed by seismic to well tie and attribute analysis. The latter was combined with seismic texture classification to increase the accuracy of seismic horizon identification. Interpolation and extrapolation of seismic characters using seismic attributes between and beyond wells here was performed by incorporation of seismic and other sources of information via Co-Kriging procedure. Nevertheless, it strongly depends on the availability of properly sampled data sets. It should be noted that, due to the simplicity of the structural modeling in the study filed and because of the large number of the available wells, the effective radius for matching correlation between well tops and picked horizons in each well was selected as 200 *m*. Time structural maps for all the selected horizons were obtained. Subsequently, velocity model building step, required for the time – depth conversion (TDC) procedure was performed. Since the TDC step is an important part of the initial interpretation, which strongly affects the result of seismic reservoir characterization, thus it is required to perform this step with the most appropriate method. In this regard, the velocity cube was prepared by four different methods and the most appropriate result was used for depth conversion and depth structural mapping. These methods were: layer-based inversion tomography, gridded inversion tomography, conventional migration velocity analysis and residual migration velocity analysis. The criteria for selecting the appropriate velocity model was the consistency of model with data and flatness of seismic events in common image gathers. Based on these criteria, the most favorable velocity model was obtained by the layer-based inversion tomography. The preference of this method was the stronger vertical heterogeneity compared to mild lateral heterogeneity. After finalizing the interpretation step, the initial inversion procedure was performed for initial modelling of acoustic impedance, especially for the main reservoir zone by genetic inversion. Then it was followed by the selection of some related attributes, such as variance, envelop and chaos for the artificial neural network estimation, after analyzing and indicating high correlation among the inversion parameters. The artificial neural network training is also required for feature classification of target formations by facies changes. According to the characteristics of seismic data and seismic facies of the target formation, various methods were proposed for artificial neural network analysis (Tenzer et al. 2010). By reducing inconsistency of the inversion result and rock properties model using well log data and/or core analysis, simple gridding, layering, zonation and geometrical modeling could be performed for enhanced inversion procedure (Soleimani and Jodeiri 2015). This procedure consists of a generating final

inversion model for acoustic impedance by the genetic inversion method, which is followed by an enhanced effective porosity modelling for target formation. The whole evaluation process could be performed by comparing the cross plot diagrams (between models and wells). For better explanation of the proposed strategy, a text flowchart of the major and minor steps comes in the following:

Prerequisites
Perform accurate seismic signal enhancements
Defining structural and diagenetic control on porosity
Perform petrophysical and seismic data adjustment
The proposed strategy
The interpretation step
Seismic structural interpretation
Well data analysis
Generation of synthetic seismogram and seismic to well tie
Attribute analysis and seismic texture classification
Interpolation and extrapolation of seismic characters in inter-well spaces
Time – depth conversion using velocity analysis
Time structural map for target horizon
Velocity model building
TDC and well control
The inversion and attributes analysis
Initial inversion procedure
Initial modelling of acoustic impedance by genetic inversion
Selection of some related attributes for the artificial neural network
Training step for feature classification by facies changes
Rock properties analysis (seismic reservoir characterization)
Reducing inconsistency using well log data and/or core analysis,
Simple gridding, layering, zonation and geometrical modeling
Generating final inversion model for acoustic impedance by the genetic inversion

The main step of the proposed strategy is using genetic algorithm and artificial neural network for genetic inversion. The proposed strategy here use artificial neural network and genetic algorithm to define the relationship and accurate parameters for accurate inversion. In the proposed strategy, artificial neural network solves the inverse problem. During this procedure, the genetic algorithm would be used to optimize the parameters, and the acoustic impedance logs were used to train the artificial neural network. The algorithm used here for artificial neural network was the back propagation algorithm, used to define a non-linear relation between the input and output data. This step initiates by selecting a small portion of data for initial optimization of inversion parameters. Then a procedure using simultaneous genetic algorithm and back propagation algorithms would be used to create the initial population, defining the genetic algorithm population and fine adjustment of parameters for the selected chromosome. This procedure will be repeated for all of the generations defined previously. Thereafter, the results would be evaluated using a fitness equation which will lead to a selection of the best chromosome. The genetic algorithm uses a stochastic procedure to attain to the final and optimum solution. Therefore, it will analyze a group of candidate solutions that were selected from a predefined initial population. In the

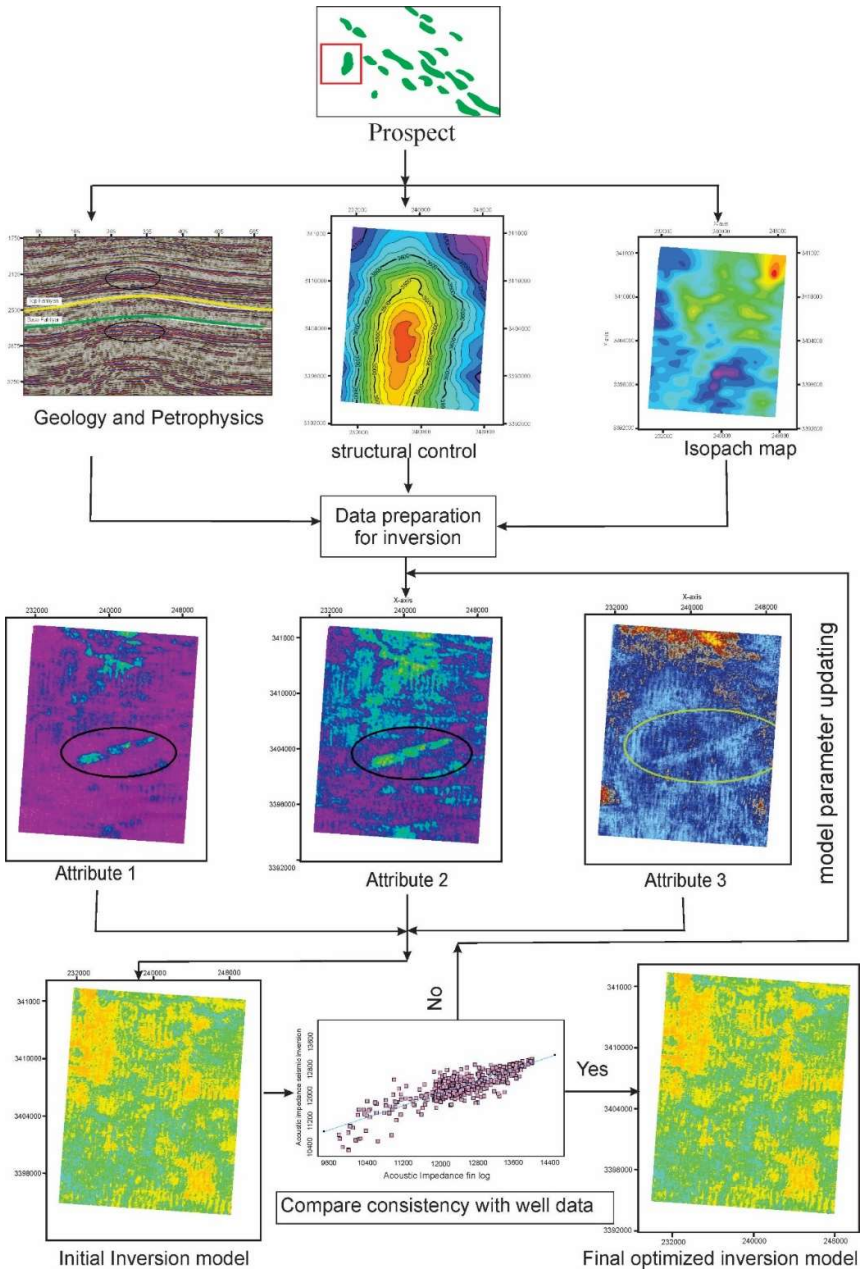

Figure 1. A simplified flowchart of the proposed strategy.

next step, the population would be improved through a new generation. This population would have candidates that would be closer to the solution with a higher probability. Any individual candidate has been selected to be analyzed as the optimal solution contains information on control variables as chromosome. The stochastic procedure that create and analyze these candidates to select the optimal solution consists of selection, crossover and mutation operators. The selection operator in the genetic algorithm is a simple roulette-wheel algorithm. However, since there is always possibility that the local optimum generation overwhelm the global optimum generation, its algorithm was improved using the elitist selection method. The selection operator will pass only the

generation whose fitness satisfy a predefined threshold to the next new generation. Then the roulette-wheel will select the rest of chromosome. The following step consists of the transformation of information between any pair of chromosome. This would be performed using a crossover operator. Exchange of information between two chromosomes could be applied for both real and binary parts using various methods, such as two-point mechanism. To attain the capability of random search through varying certain genes of chromosome, a mutation operator should be defined. This is a simple procedure, which selects a chromosome and randomly defines another one for exchange of their information. As a general remark, the conventional genetic algorithm uses random mechanism in crossover and mutation operators. However, they could be improved to adaptive or dynamic mechanism. This method will define the probability of crossover and mutation based on the fitness value of the solution.

The stepwise procedure on applying the genetic algorithm in this study
Standardize raw data, seismic and well logs
Initialize population, pop-size, maximum generation (Maxgen), gen=0
Generate initial population
Evaluate fitness
Calculating and applying the genetic algorithm and operators
Fine adjustment of parameters via artificial neural network for the selected chromosome
gen=gen+1
gen equals the Maxgen?
If No, select the next generation and fitness evaluation
If Yes , follow the chart
Best chromosome
Extract appropriate and optimized parameters for inversion and porosity estimation
Evaluate porosity model with the core analysis data and thin section

3 The study area

The study field is a symmetric elongated anticline structure situated in the south west of Iran, in Dezful embayment (Figure 2a). Production from field is performed from the Fahlyian reservoir, mainly from fractured carbonates. The structural trend of the petroleum field (N-S) is different from the main trend of petroleum fields in the Zagros fold thrust belt, which is mainly (NW-SE) (Ghanadian et al. 2017; Derikvand et al. 2018; Farshi et al. 2019). The main purpose of the 3D seismic acquisition was an investigation on the reservoir characteristics of Ilam, Sarvak and Fahlyian formations (figure 2b) (Movahed et al. 2015). The target reservoir formations, which are Sarvak and Fahlyian formations, were investigated in previous studies for different litho-facies. Due to the lack of core sample, thin sections obtained from drilling cuttings were used. Nevertheless, they were sufficient for separation of different porosities for further porosity mapping in the proposed inversion analysis. The facies in the target formation consist of very fine to fine grained mudstone and wackestone containing a pelagic biota, set in a micrite matrix-cemented limestone. This litho-facies in the lowermost part of Sarvak formation possesses low porosity with 5-15% micro-porosity in the matrix, (Dehkar et al., 2018).

4 Application of the proposed strategy to the selected reservoir

The study area was investigated by acquisition of 3D seismic data to increase understanding of the subsurface geology. Table 1 shows the acquisition parameters

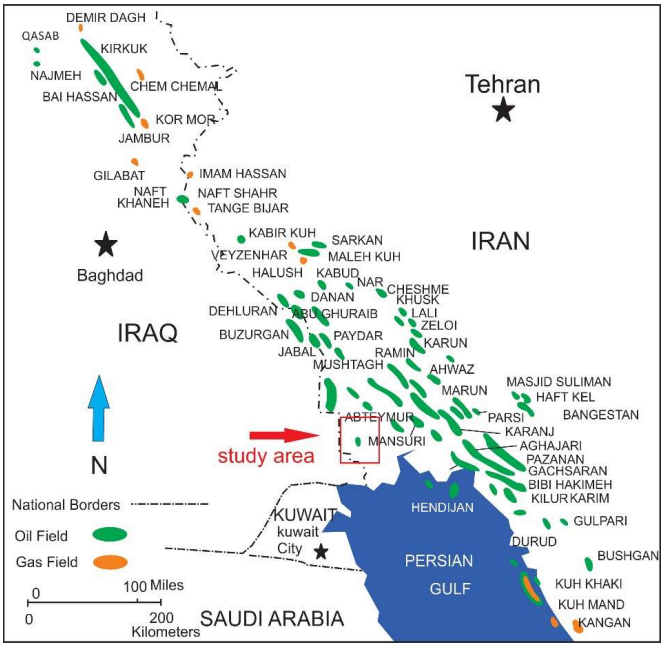

(a)

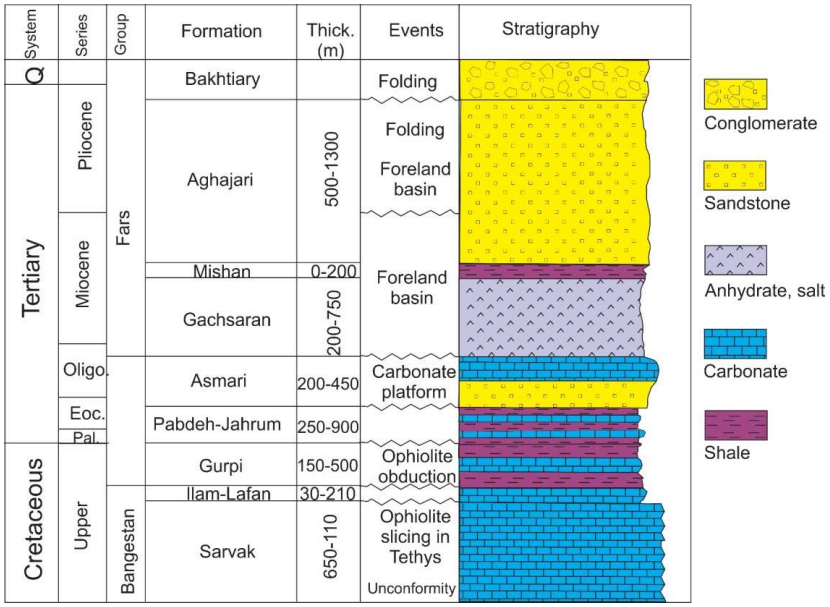

(b)

Figure 2. (a) Location of the study reservoir in the southwest of Iran. (b) stratigraphy of the selected study area (Soleimani 2017a).

of the used 3D seismic dataset. Selecting a desired orientation, such as the vertical sections along the dominant dip direction, will ascertain the structural pattern of the field study. Time slices may then be studied to check out the accuracy of the structural modelling. Locally, for the tertiary and cretaceous interval, subjected to multiple erosional phases, intermediate horizons were picked with the objective to evaluate all the possibilities of subsidiary play. The use of 3D seismic data allowed both structural and stratigraphic variations to be imaged and the locations of previous wells to be better evaluated. However, it requires the generation of synthetic

seismogram for appropriate well log analysis and inversion. The essential requirements for the generation of synthetic seismogram are velocity and density logs, where the final product is the zero-offset seismic trace.

Table 1. Key data acquisition parameters for the 3D survey in the study area.

Acquisition parameter	Value	Acquisition parameter	Value
Area	382 km^2	Low cut filter	2Hz
Number of shots	16992	High cut filter	125 Hz
Number of swathes	42	Sources point interval	50 m
Bin size	25m × 25m	Source line interval	450 m
Nominal multiplicity	16 fold	Receiver interval	50 m
Number of channels	144×4	Receiver line interval	300 m
Sample rate	2 ms	Patch	4×144
Record length	6 sec	Total channels	576

The principal deficit in making synthetic seismogram is that the input data are commonly incomplete. Reliable density data are often missing over the most of the boreholes, but this is not a severe handicap because the density usually varies in the same way as the velocity does. Hence, there may be errors in calculating the arrival time of an event even though the prediction of the wave shape is adequate. Discrepancies between the arrival time of an event on a synthetic seismogram and the one observed on a seismic record can be also produced by filter delays in recording and/or processing using different reference datum (Soleimani et al. 2016). Based on synthetic seismograms and well markers, the top and the base of the interested lithological units were selected for picking the horizons throughout the whole 3D cube with some subsidiary horizons (Figures 3a and 3b). The Gachsaran formation, which is mainly evaporite and partly marl in the study area, is depicted as a strong and continuous reflector in seismic images. As it was assumed, the two-way time map shows that there is no structural closure at the top of the Gachsaran formation and its general dip is toward the NE. However, a flexure with N-S trend in the location of the study structure can be seen at the time map. The Asmari formation, which is mainly limestone (Ghar or Ahwaz Member) and partly carbonate in the study area, is illustrated more or less as a continuous reflector in seismic data. The two-way time map of the Asmari formation shows that there is no structural closure at the top of the Asmari level, and its general dip is toward to the NE. Stream features are evident in the attribute maps of the Asmari formation (not shown here). Their trend is in coincidence with the overall direction of sediment transportation from SW to NE. In addition, a lineament with NW trend affects the top of the Asmari formation. It could be representative of a sub-seismic fault or deflection line on sedimentary basin (Zhao et al. 2018). Through the seismic interpretation, the Ilam formation was interpreted as a strong reflector due to its large acoustic contrast with the Gurpi shale formation. Analysis of various seismic attributes revealed lineaments on top of the Ilam formation. It was assumed that these features are small deflections related to the sedimentary features especially in buildup type. The Sarvak formation is a thick and mostly carbonate layer in the study area, which could be differentiated into two sub-horizons, based on the seismic attributes.

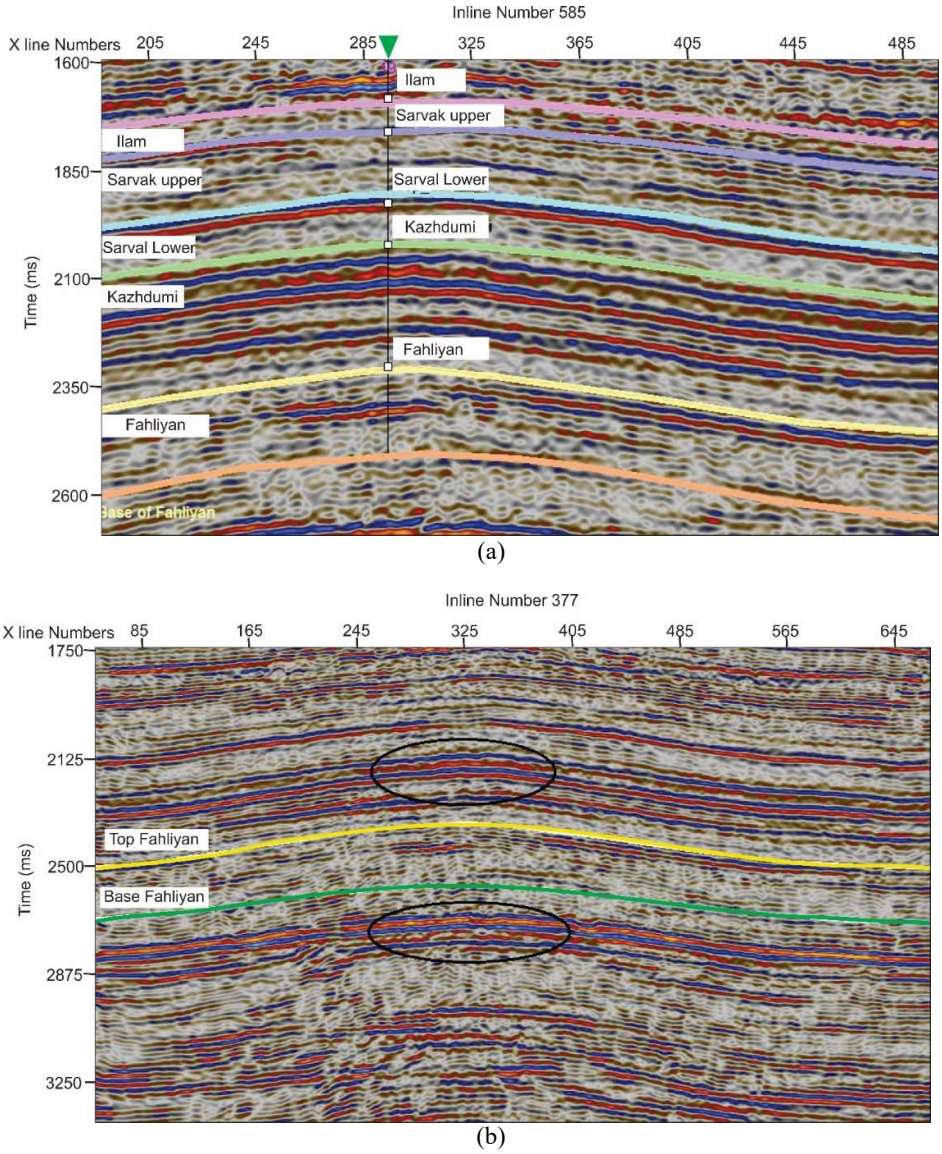

Figure 3. (a) An inline of 3D seismic data from the study area shows the sequences of the study area. (b) another seismic image example of the data shows the anticline structure of the reservoir inline.

The upper horizon represents an erosional unconformity, which was depicted by variations in reflectivity along the erosional channel. The lower part of the Sarvak horizon shows characters of a favorable reservoir. The western flank of this section depicts a gentle dip while seismic reflectors show downlap features. The Fahlyian formation, which is another target formation in this study, is known as the main reservoir. Same as the Sarvak formation, the Fahlyian formation here was also divided into two members. The upper Fahlyian represents more or less a basinal facies characteristic, while the lower Fahlyian depicts shelf carbonate facies. Attribute analysis of the target formation was performed by an artificial neural network and indicates trends of some obvious lineaments which are probably related to sedimentary features (Figure 4). The seismic attributes that were used in this study are variance, envelope and chaos, which show the properties of the target formation. Table 2 shows the correlation values between the attributes which defines the importance of the weighting for each attribute in further

integration. Values in table 2 present the correlation between different seismic attributes to obtain the most appropriate combination attribute. Values in the last row, which are total values, are physically or geophysically meaningless correlations values. However, they presents somehow some meaning as if we use a combination of the attributes in all rows with the attribute in the selected column, the correlation values would be the same in the total row. The value is high in the total row, since all the irrelevant and uncorrelated attributes influence on this value. Figure 4d shows the result of the integration of surface attributes applied on those obtained attributes which could be used for further evaluation of the reservoir characteristics. The combined attribute image in figure 4d was obtained based on the correlation values in Table 2. Correlation between seismic attributes and reservoir parameters, and the correlation between different seismic attributes are useful evaluation parameter for selection of the appropriate seismic attributes. To select the most appropriate attributes, a group of large number of attributes would be selected based on the correlation between the seismic attributes and the reservoir parameters. Generally, some types of seismic attributes would be initially selected, which shows high correlation with reservoir parameters. An

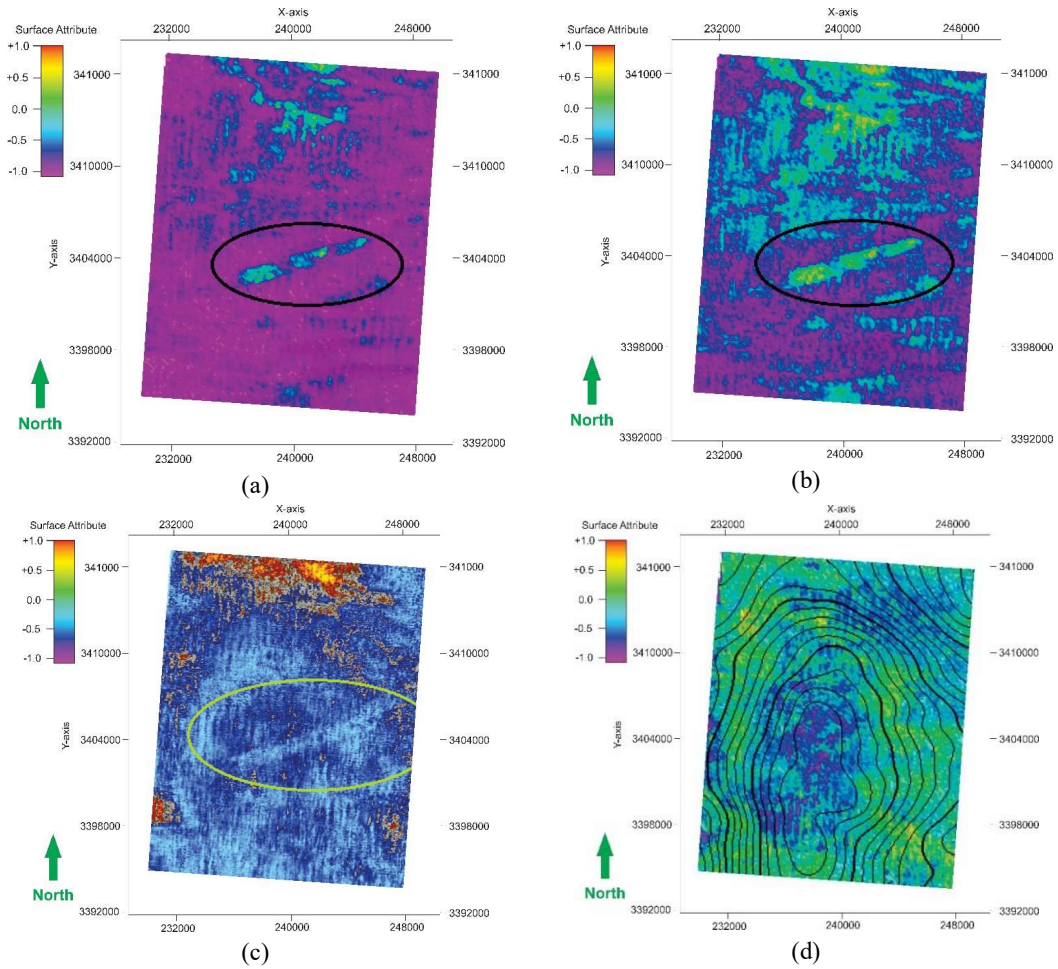

Figure 4. (a) A time slice of the variance attribute of the target formation that shows a lineament in the target. (b) The chaos attribute of the same time that shows chaotic pattern of the study reservoir. (c) the envelope attribute that shows the same lineament and the reservoir structure. (d) the combined attribute image which was obtained based on the correlation values in Table 2.

Table 2. Correlation between different seismic attributes to obtain the most appropriate combination of attributes

	Variance	Envelope	Chaos
Variance	1.0000	0.3953	0.4638
Envelope	0.3953	1.0000	0.5207
Chaos	0.4638	0.5207	1.0000
Total	0.4975	0.5489	0.5916

additional step is also required to remove redundant attributes and reduce the number of seismic attributes used for reservoir prediction. There might be a high correlation value between the selected seismic attributes, and thus seismic attributes with higher correlation values might be clustered into one category. These studies have been previously performed and it is not a complicated issue to select the appropriate attributes for any special purpose (Gao et al. 2006; Qi and Zhang, 2012; Galvis et al. 2017). Previous studies has shown that the selected attributes in table 2 are the appropriate attributes for the selected purpose and their low correlation values in table 2 reveals that they could be integrated to provide the unique attribute.

After the interpretation of seismic data, it is required to perform velocity analysis to derive the depth map from time structural data. Due to the heterogeneity of the study reservoir, care should be taken to use a velocity analysis strategy which shows capabilities in handling lateral velocity changes (Motamedi et al. 2012). Thus, here we performed velocity analysis in three steps. Initially, we have performed prediction of an optimal seismic velocity field derived from pre-stake seismic data. Subsequently, a general statistical analysis was used to produce an integrated interval velocity field. This velocity should provide the best possible well to seismic tie, while being sufficiently smooth for proper migration. Appropriate velocity model was selected based on the calculation of the velocity errors and the inconsistency between the velocity model and data. This procedure was repeated until a satisfactory velocity model was obtained. It should be noted that this strategy was performed by four different initial velocity models which were stacking velocity, average velocity, interval velocity and well derived velocity. Subsequently, depth structural model was derived based on the most appropriate depth model, according to the least misfit with well data. Afterwards, the proposed strategy for the reservoir characterization could be applied on the structural depth model and perform the inversion procedure using the artificial intelligent method. Figure 5 shows an underground counter depth map of the target formations (Sarvak and Fahlyian) which shows a gently dipping anticline that has formed the oil trap in the study field. To provide a better image of the structural traps, isopach maps of the target formations were derived (Figure 6), which depicts the thickness of the petroleum column. A combination of these maps, with the final inversion result, could be used for further appraisal study of the reservoir (Presho et al. 2011).The common method for seismic inversion is the deterministic post stack inversion, while the stochastic inversion on pre-stack data provides the most accurate result. We have used the result of this method for comparing the result obtained by the proposed strategy. The proposed strategy uses an artificial neural network system and genetic algorithm in order to provide an accurate seismic property cube. As it

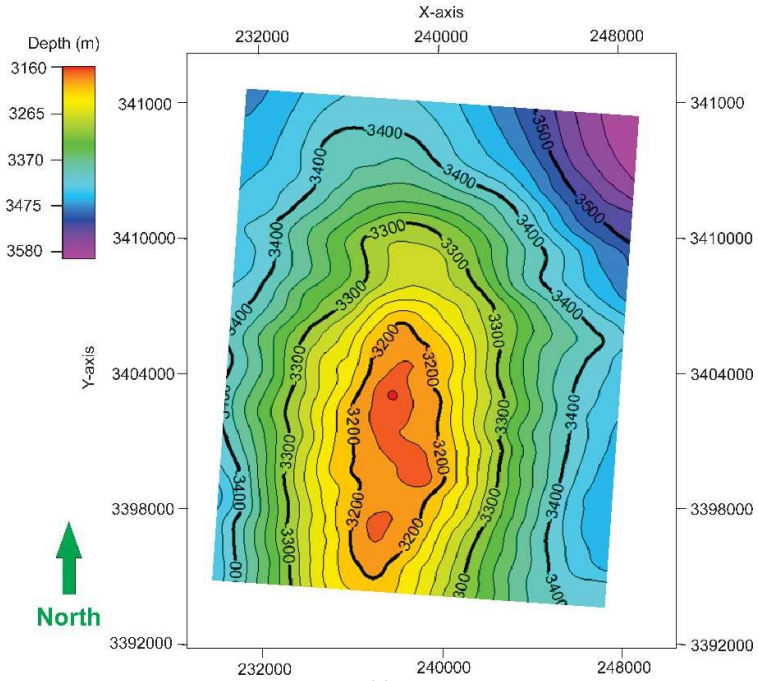

Figure 5. (a) Depth structural model of the first target formation (Sarvak) in the study reservoirs and (b) depth structural model of the other target formation (Fahlyian). Both structural models show an anticline in the study area with gentle dips.

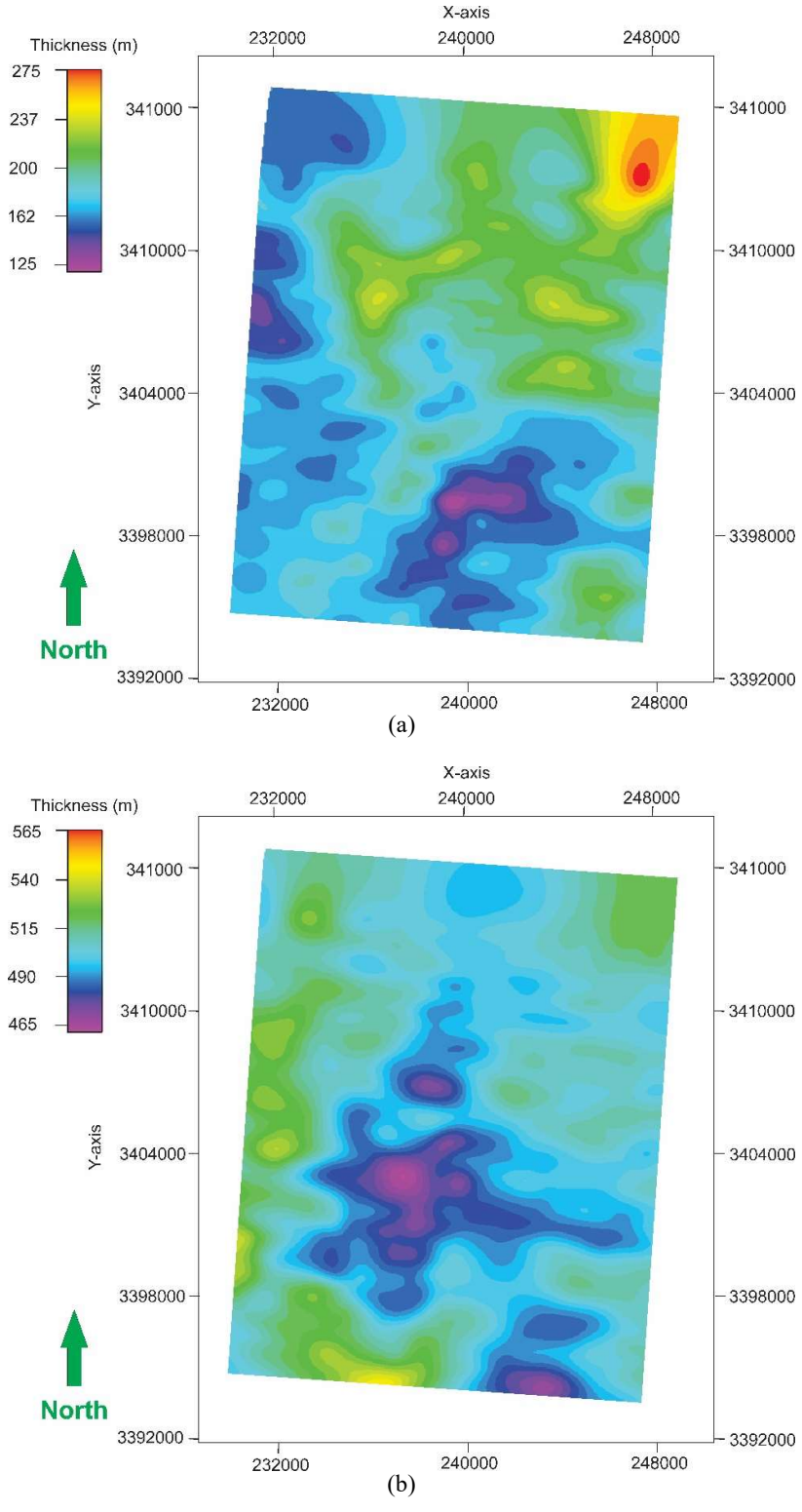

Figure 6. (a) Isopach map of the first target formation (Sarvak) in the study reservoirs and (b) isopach map of the other target formation (Fahlyian). Both maps show the thickness of the oil column in the target formations.

was shown in the flowchart of the proposed strategy (Figure 1), this algorithm does not require to generate the synthetic seismogram like the conventional model based, sparse spike and band limited seismic inversion methods (Hu et al. 2017). The proposed method uses the genetic algorithms and/or algorithms of the back propagation for definition of the error in a non-linear manner. Normally, the linguistic variables and the maximum number of the generations have to be predefined. These values were defined using a sensitivity analysis and visual inspection of the result. However, it should be noted that this is a very time-consuming procedure to select a wide range of these parameters and define the optimum values. Therefore, this step was performed on a small selected cube of data and narrow range with sparse values. Finally, the selected values for linguistic variables were defined as 10, the population size was defined as 35 and the maximum generation was selected as 165. The training and validation errors, as the result of applying the artificial neural network for the data example could be seen in table 3. Also the cross correlation and the average error were also revealed in table 3.

Table 3. Training and validation error for the selected data set. The cross correlation and average errors were also depicted.

Attribute	Training error	Validation error	Validation result		Application result	
			Cross correlation	Average error	Cross correlation	Average error
Acoustic Impedance	0.0421	0.0352	0.7854	0.1021	0.6985	0.1706
Amplitude Envelope	0.0318	0.0411	0.7120	0.1108	0.7243	0.1912
Chaos	0.0335	0.0352	0.6988	0.1802	0.7158	0.2011
Structural smooth	0.0508	0.0511	0.6842	0.1816	0.6719	0.1714
Smoothing Variance	0.0384	0.0398	0.7235	0.1632	0.7533	0.1832

Inversion procedure was performed in two windows in accordance with 3D seismic data recalculated in depth domain. The result of the inversion procedure was used to obtain an acoustic impedance volume which was subsequently used for porosity prediction in the cross-well space. Generally, the results of the seismic inversion procedure are appropriate for the prediction of physical properties of the media in the cross-well space (Sentenac et al. 2018). Evaluation of the inversion result was simultaneously carried out by means of well data reproducibility in accordance with seismic data. At the first step of the evaluation, the acoustic impedance data in some wells were involved in the artificial neural network training during the inversion. Subsequently, independency of variables during the inversion procedure, which was performed and calculated individually for each sub-volume of data by means of 3D seismic cube and well data, was carried out by cross plots and related interdependency diagrams. At the second step of this simultaneous inversion procedure, the acoustic impedance cube was calculated by taking into account all the available 3D seismic and well data. It should be noted that the acoustic impedance cube was re-scaled into geological model and applied for porosity prediction into cross-well space (Norden et al. 2012). Figure 7a and 7b show the inversion results for the Sarvak formation by the conventional method and the proposed strategy, respectively. Same

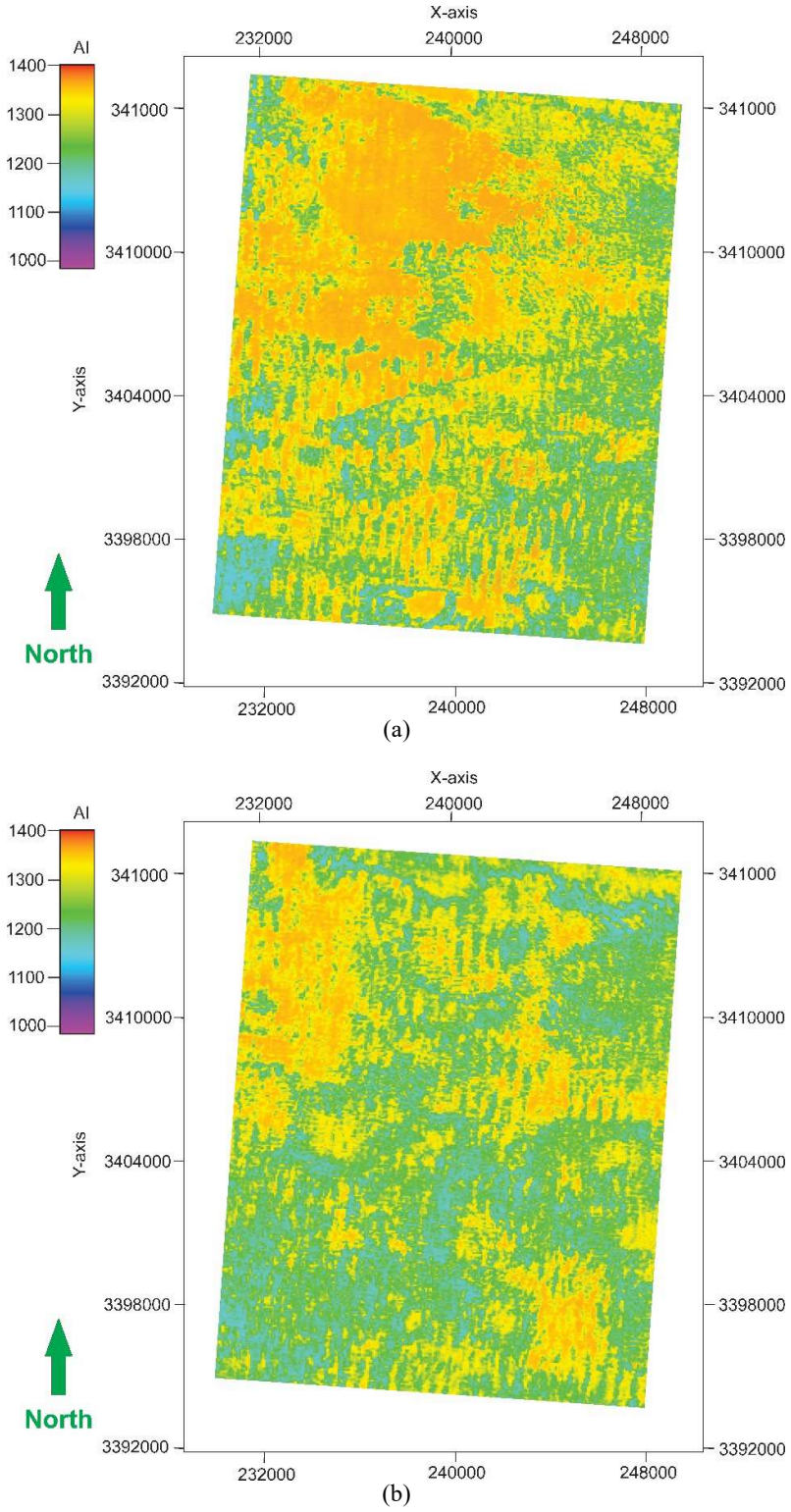

Figure 7. Results of the inversion for the Sarvak formation (a) by the conventional method and (b) by the proposed strategy.

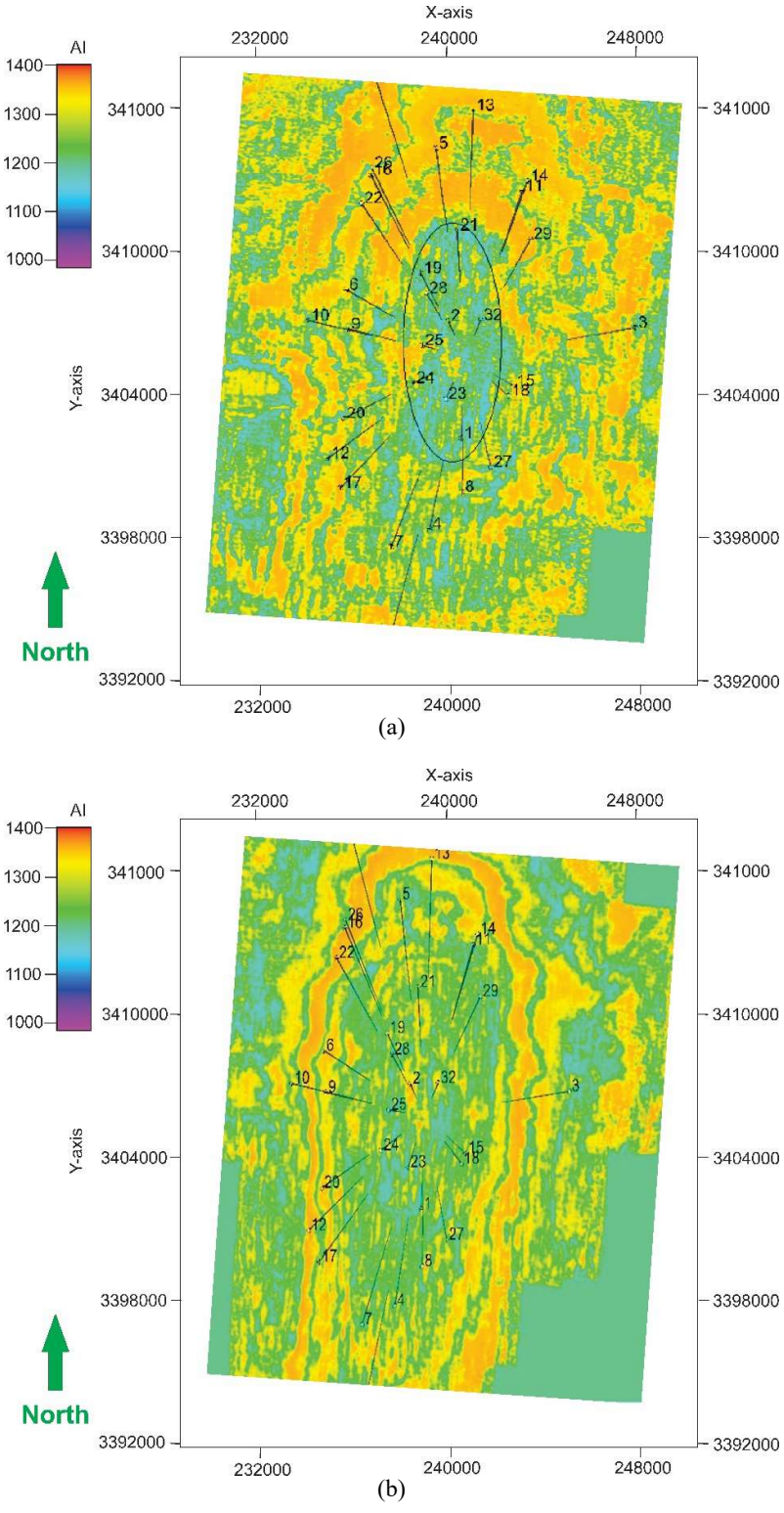

Figure 8. Results of the inversion for the Fahlyian formation (a) by the conventional method and (b) by the proposed strategy.

results, for the Fahlyian formation are also shown in figure 8. As it could be seen, the proposed strategy increases the resolution of the inversion result. However, accuracy of the result could not be evaluated independently, but the porosity model could be derived from each inversion result. Evaluating the porosity model with well data could define the accuracy of each inversion result. Reservoir porosity prediction was performed here for the Sarvak and the Fahlyian formations based on the result that was obtained by the genetic inversion. Figures 9a and 9b show the porosity model for the Sarvak formation derived from the result of the conventional inversion and the proposed strategy, respectively. The same procedure was performed for the Fahlyian formation and the porosity model for this target is illustrated in Figure 10. Obviously, the proposed method could increase the resolution of the final images, while the conventional method for both target formations suffers from less precise distribution of porosity. Table 4 shows the correlation values which were obtained during the procedure of the genetic inversion using seismic attributes for the evaluation procedure. For better understanding of variation in acoustic impedance and the effective porosity, a 2D arbitrary line from the study field was selected for illustration. Figure 11a shows the arbitrary line illustrating the variation of acoustic impedance obtained by the genetic inversion in the study field. The same arbitrary line for the effective porosity is also presented in figure 11b. The results of porosity genetic inversion in this study were evaluated here by a linear regression analysis. Figure 12a shows a simple regression for porosity values obtained by the proposed method versus its values in well data for the Sarvak formation in well number 2. Figure 12b shows the same regression for the Fahlyian formation in the same well. As it could be seen, high correlation values in both cases, confirms the accuracy of the porosity estimation by the genetic inversion.

For better evaluation, we also defined the correlation values and the RMS error for the inversion step and the model evaluation respectively. Tables 5 and 6 show the correlation values for the acoustic impedance, effective porosity and the QC well, as well as the RMS error for the porosity model with well data for Sarvak and Fahlyian formation, respectively.

Table 4. Correlation values between used attribute for inversion evaluation and the final result of the genetic inversion.

	Acoustic Impedance	Envelope	Chaos	Structural smooth	Smoothing variance	Genetic Inversion
Acoustic Impedance	1.0000	0.0035	0.0027	0.2185	0.0015	0.0122
Envelope	0.0035	1.0000	0.4231	0.0047	0.3304	0.1068
Chaos	0.0027	0.4231	1.0000	0.0065	0.5530	0.2910
Structural smooth	0.2185	0.0047	0.0065	1.0000	0.0055	0.0027
Smoothing variance	0.0015	0.3304	0.5530	0.0055	1.0000	0.4229
Genetic Inversion	0.0122	0.1068	0.2910	0.0027	0.4229	1.0000
Total	0.2189	0.4427	0.6129	0.2187	0.6301	0.4384

Table 5. Correlation values in the learning step and application of the artificial neural network for acoustic impedance and effective porosity, the correlation value for selected evaluation wells and the RMS values for porosity estimation between values obtained by the proposed method and well logs, for Sarvak formation.

Model	Total Correlation in learning step	Well Number	Correlations in application	Samples
Acoustic Impedance	0.8576708	Created predicted log for well: 24	0.850686	580
		Created predicted log for well: 10	0.7849868	565
		Created predicted log for well: 16	0.7358335	585
		Created predicted log for well: 14	0.7921326	585
Effective Porosity	0.7673773	Created predicted log for well: 24	0.8666095	593
		Created predicted log for well: 10	0.8033919	530
		Created predicted log for well: 16	0.8106907	588
		Created predicted log for well: 14	0.8558064	580
QC wells	0.8138589	Created predicted log for well: 32	0.8117909	112
		Created predicted log for well: 13	0.7817909	593
The RMS value for effective porosity between proposed strategy and well data for well 10.			1.67	
The RMS value for effective porosity between proposed strategy and well data for well 14.			2.25	
The RMS value for effective porosity between proposed strategy and well data for well 16.			0.98	
The RMS value for effective porosity between proposed strategy and well data for well 24.			0.68	

Table 6. Correlation values in learning step and application of the artificial neural network for acoustic impedance and effective porosity, the correlation value for evaluation wells and the RMS values for porosity estimation between values obtained by the proposed method and well logs, for the Fahlyian formation.

Model	Total Correlation in learning step	Well Number	Correlations in application	Samples
Acoustic Impedance	0.8576708	Created predicted log for well: 9	0.7781889	40
		Created predicted log for well: 5	0.6118608	30
		Created predicted log for well: 4	0.4347483	30
Effective Porosity	0.7673773	Created predicted log for well: 9	0.8277186	51
		Created predicted log for well: 5	0.7106792	53
		Created predicted log for well: 4	0.5638568	55
QC well	0.7523684	Created predicted log for well: 8	0.1432808	48
The RMS value for effective porosity between proposed strategy and well data for well 4.			1.32	
The RMS value for effective porosity between proposed strategy and well data for well 5.			1.12	
The RMS value for effective porosity between proposed strategy and well data for well 9.			0.98	

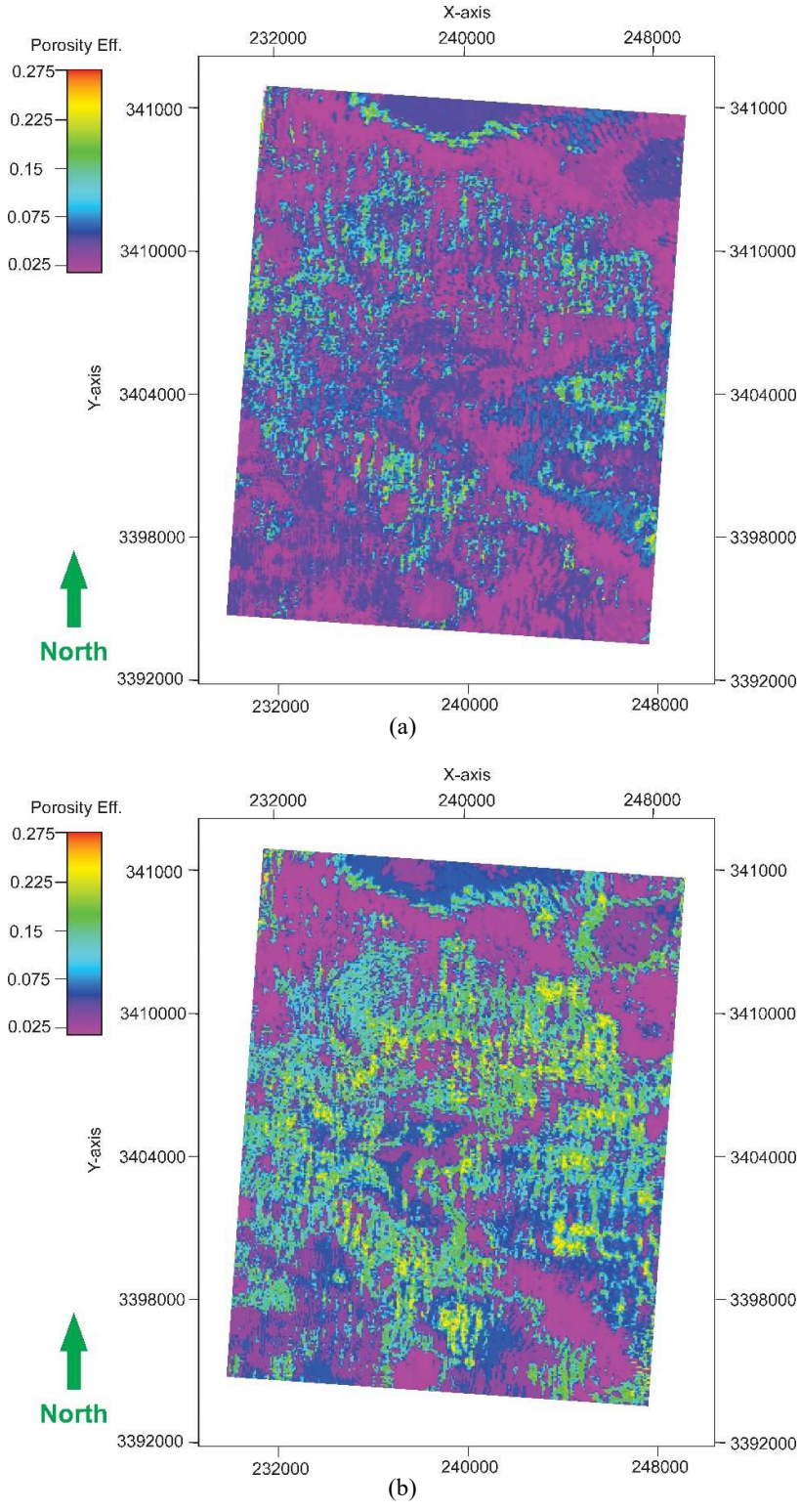

Figure 9. Results of the porosity model for the Sarvak formation (a) by the conventional method and (b) by the proposed strategy.

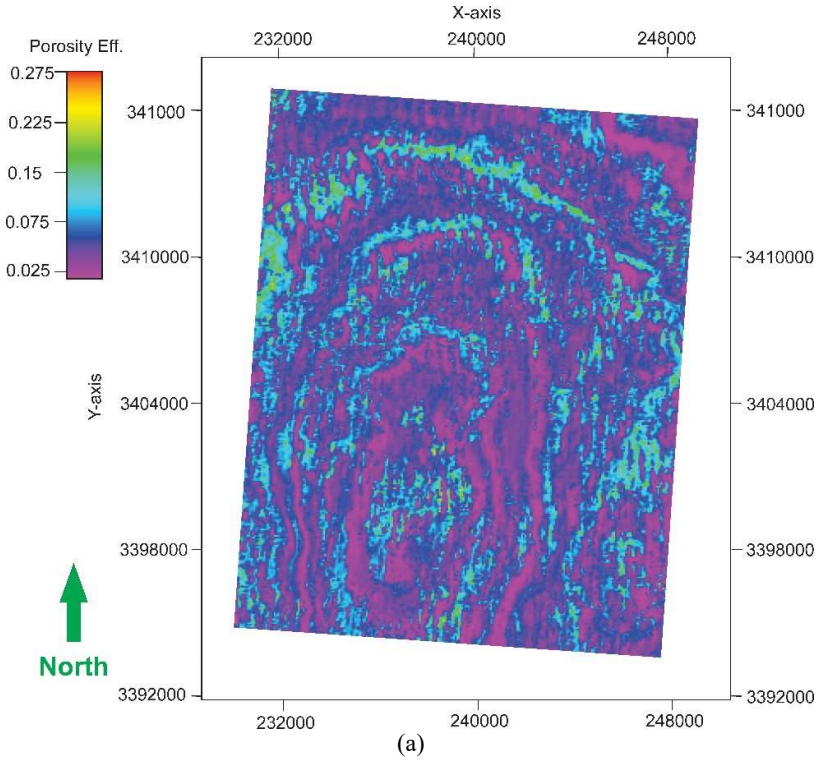

Figure 10. Results of the porosity for the Fahlyian formation (a) by the conventional method and (b) by the proposed strategy.

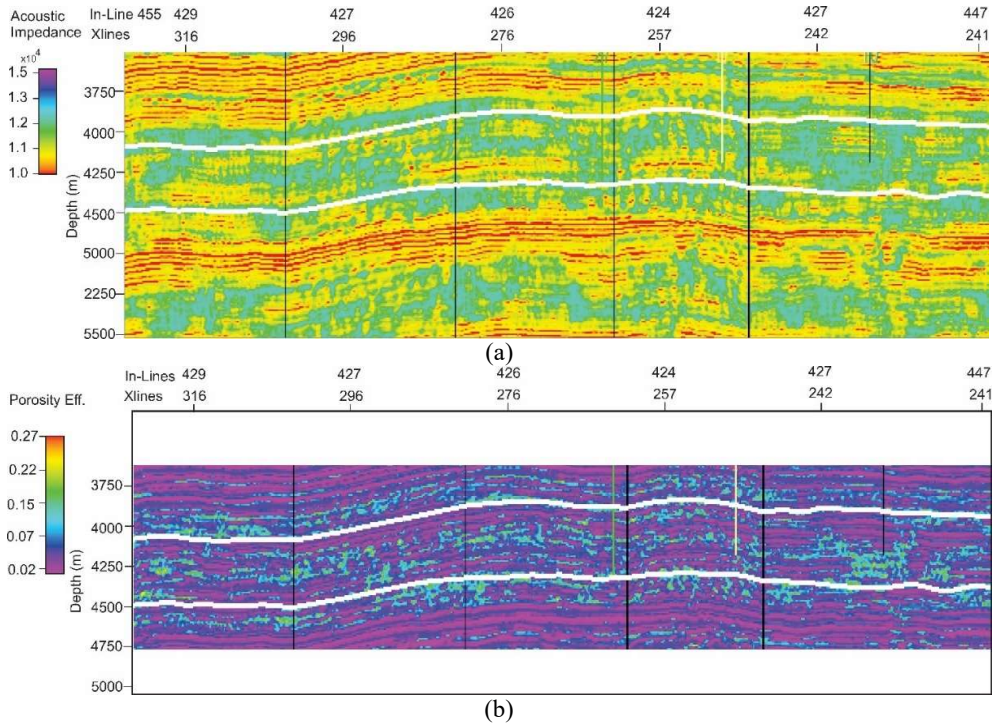

Figure 11. (a) A vertical 2D arbitrary line of the study field presenting the acoustic impedance obtained by the genetic inversion. (b) A vertical 2D arbitrary line of the study field showing the effective porosity. The Fahlyian formation is showing by white lines on the sections.

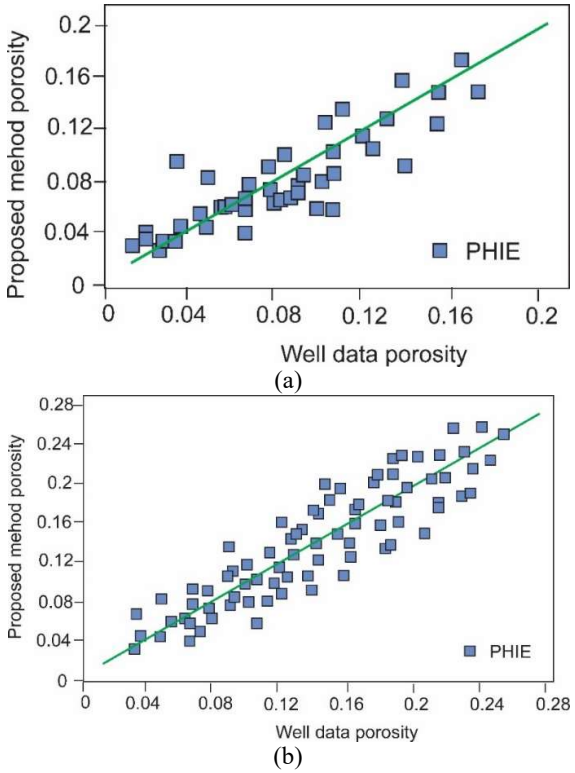

Figure. 12 (a) The simple linear regression for the porosity estimated by the proposed method versus the conventional method for the Sarvak formation and (b) the simple linear regression for the porosity estimated by the proposed method versus the conventional method for the Fahlyian formation. Both regression lines were derived using data from well number 2, in the center of the reservoir.

5 Conclusion

The proposed inversion strategy, which consists of an integration procedure of the conventional inversion procedure using an artificial neural network analysis and a genetic inversion, could resolve some of the ambiguities in the conventional inversion. The procedure, however, requires accurate interpretation both in structural analysis and seismic reservoir properties. In the presented study, the interpretation of seismic data and structural modelling revealed that the study reservoir is situated as a gentle elongated anticline, which was not strongly affected by tectonic condition. Therefore, it was supposed that the the lateral lithofacies changes plays an important role in the creation of possible stratigraphic traps. The upper member of the Sarvak formation indicated two parallel series of buildups with ENE-WSW trends. In the trough between two parallel seismic features down-lapping reflectors was considered as stratigraphy sedimentary features within a small intra-platform depression. Inversion results in the lower part of the Fahlyian formation also indicated good to fair porosity distribution using the proposed strategy. High correlation value between the acoustic impedance and the porosity was observed in the Fahlyian formation. Comparison of inversion result and porosity models for two reservoirs with different rock types revealed that the proposed inversion strategy exhibits accurate performance in the carbonate intervals.

References

Abdel-Rasoul RR. Daoud A. El-Tayeb E.S.A. (2014) Production allocation in multi-layers gas producing wells using temperature measurements with the application of a genetic algorithm, Pet. Sci. Tech. 2014; 25-28 https://doi.org/10.1080/10916466.2011.586958

Ahmadi MA. Soleimani R. Lee M. Kashiwao T. Bahadori AR. (2015) Determination of oil well production performance using artificial neural network (ANN) linked to the particle swarm optimization (PSO) tool. Pet., 1(2), 118-132; https://doi.org/10.1016/j.petlm.2015.06.004

Al-Bulushi, N.I., King, P.R., Blunt, M.J., Kraaijveld, M., (2012) Artificial neural networks workflow and its application in the petroleum industry: Neural Comp and Appl, 21 (3), 409-421 https://doi.org/10.1007/s00521-010-0501-6

Balouchi, S., Moradi, S., Masihi, M., Erfaninia, A.A., (2013) A Novel combinatorial approach to discrete fracture network modeling in heterogeneous media. Iranian Journal of Oil and Gas Sci and Tech, 2(1), 42-56. https://doi.org/10.22050/IJOGST.2013.3037

Benisch, K., Köhn, D., al Hagrey, S., Rabbel, W., Bauer, S., (2015) A combined seismic and geoelectrical monitoring approach for CO2 storage using a synthetic field site. Environ Earth Sci. 73(7) 3077–3094, https://doi.org/10.1007/s12665-014-3603-0

Chen, Y., Durlofsky, L.J., (2006) Adaptive local-global upscaling for general flow scenarios in heterogeneous formations, Tran Por Med, 62(2), 157-185. https://doi.org/10.1007/ s11242-005-0619-7

Daraei M, Bayet-Golla A, Ansari M, (2017) An integrated reservoir zonation in sequence stratigraphic framework: A case from the Dezful Embayment, Zagros, Iran. J of Petro Sci and Eng. 154, 389-404, https://doi.org/10.1016/j.petrol.2017.04.038

Dehkar, A., Sajjadian, V.A., Noora, M.R.,

and Shabani Goorji, K., (2018). Microfacies analysis and depositional environment of the Fahliyan Formation (Lower Cretaceus), Abadan plain, West South of Iran (Arvand-feld). Geosciences, 106, 45-52.

Derikvand B, Alavi A, Abdollahie Fard I, Hajialibeigi H, (2018) Folding style of the Dezful Embayment of Zagros Belt: Signatures of detachment horizons, deep-rooted faulting and syn-deformation deposition. Mar and Petr Geo. 91, 501-518. https://doi.org/10.1016/j.marpetgeo.2018.01.030

Farshi M, Moussavi-Harami, R, Mahboubi A, Khanehbad M, Golafshani T, (2019) Reservoir rock typing using integrating geological and petrophysical properties for the Asmari Formation in the Gachsaran oil field, Zagros basin. J of Petr Sci and Eng.176, 161-171. https://doi.org/10.1016/j.petrol.2018.12.068

Galvis I, Villa Y, Duarte C, Sierra D, Agudelo W., (2017) Seismic attribute selection and clustering to detect and classify surface waves in multi-component seismic data by using k-means algorithm. The Leading Edge, 33(6), 239–248. http://dx.doi.org/10.1190/tle36030239.1.

Gao J, Wang J, Yun M, Huang B, Zhang G, (2006) Seismic attributes optimization and application in reservoir prediction. Applied Geophysics. 3, 243–247. http://dx.doi.org/10.1007/s11770-006-4007-z

Ghanadian M, Faghih A, Abdollahie Fard I, Kusky T, Maleki M, (2017) On the role of incompetent strata in the structural evolution of the Zagros Fold-Thrust Belt, Dezful Embayment, Iran. Mar and Petr Geo. 81, 320-333, https://doi.org/10.1016/j.marpetgeo.2017.01.010

Guerriero V, Mazzoli S, Iannace A, Vitale S, Carravetta A, Straussc C. A., (2012), Permeability model for naturally fractured carbonate reservoirs. Mar petrol Geol. 40, 115-134, https://doi.org/10.1016/j.marpetgeo.2012.11.002

Hu, Y., Li, Z., Zhao, J., Tao, Z., Gao, P., (2017) Prediction and analysis of the stimulated reservoir volume for shale gas reservoirs based on rock failure mechanism. Environ Earth Sci. 76:546, https://doi.org/10.1007/s12665-017-6830-3

Iliev O. Rybak I. (2008) On numerical upscaling for flows in heterogeneous porous media. Comp. Meth. In App. Math. 8(1), 60-76, https://doi.org/10.2478/cmam-2008-0004.

Maffucci R, Bigi S, Corrado S, Chiodi A, Di Paolo L, Giordano G, Invernizzi C, (2015) Quality assessment of reservoirs by means of outcrop data and discrete fracture network models: The case history of Rosario de La Frontera (NW Argentina) geothermal system. Tectonophysics, https://doi.org/10.1016/j.tecto.2015.02.016

Movahed Z, Junin R, Amiri Bakhtiari H, Safarkhanlou Z, Movahed AA, Alizadeh, M, (2015) Introduction of sealing fault in Asmari reservoir by using FMI and RFT in one of the Iranian naturally fractured oil fields. Arab J Geosci, 8(12), 10919-10936. https://doi.org/10.1007/s12517-015-1951-z

Motamedi H, Sherkati S, Sepehr M, (2012) Structural style variation and its impact on hydrocarbon traps in central Fars, southern Zagros folded belt, Iran. J of Stru Geo. 37, 124-133, https://doi.org/10.1016/j.jsg.2012.01.021

Noorbakhsh SS, Rasaei MR, Heydarian A, Behnaman H, (2014) Single-phase near-well permeability upscaling and productivity index calculation

methods. Iranian J of Oil and Gas Sci and Tech, 3(4), 55-66. https://doi.org/10.22050/IJOGST.2014.7522

Norden, B., Förster, A., Behrends, K., Krause, K., Stecken, L., Meyer, R., (2012) Geological 3-D model of the larger Altensalzwedel area, Germany, for temperature prognosis and reservoir simulation. Environ Earth Sci. 67(2), 511–52. https://doi.org/10.1007/s12665-012-1709-9

Nozohour-leilabady, B. Fazelabdolabad, B. (2015), On the application of Artificial Bee Colony (ABC) algorithm for optimization of well placements in fractured reservoirs; efficiency comparison with the Particle Swarm Optimization (PSO) methodology. Petroleum, 2(1), 79-82. https://doi.org/10.1016/j.petlm.2015.11.004

Oyeyemi KD, Olowokere MT, Aizebeokhai AP (2019). Prospect analysis and hydrocarbon reservoir volume estimation in an exploration field, shallow offshore Depobelt, western Niger delta, Nigeria. Nat Resour Res., 28(1), 173-185. https://doi.org/10.1007/s11053-018-9377-4

Presho M, Woc S, Ginting V. (2011) Calibrated dual porosity, dual permeability modeling of fractured reservoirs. J Petrol Sci Eng., 77(3-4), 326-337, https://doi.org/10.1016/j.petrol.2011.04.007

Qi X, Zhang S, (2012) Application of seismic multi-attribute fusion method based on D-S evidence theory in prediction of CBM-enriched area. App. Geoph. 9, 80–86. http://dx.doi.org/10.1007/s11770-012-0317-5

Sentenac, P., Benes, V., Keenan, H., (2018) Reservoir assessment using non-invasive geophysical techniques. Environ Earth Sci. 77:293 https://doi.org/10.1007/s12665-018-7463-x

Soleimani, M., Jodeiri, B., (2015) 3D static reservoir modeling by geostatistical techniques used for reservoir characterization and data integration. Environ. Earth Sci, 74, 1403–1414. http://dx.doi.org/10.1007/s12665-015-4130-3

Soleimani M, Jodeiri B, Rafie M, (2016), Integrated petrophysical modeling for a strongly heterogeneous and fractured reservoir, Sarvak Formation, SW Iran. Nat Reso Res. 26(1) 75-88. http://dx.doi.org/10.1007/s11053-016-9300-9

Soleimani M, (2017a), Well performance optimization for gas lift operation in a heterogeneous reservoir by fine zonation and different well type integration. J of Nat Gas Sci and Eng, 40, 277-287. http://dx.doi.org/10.1016/j.jngse.2017.02.017

Soleimani M, (2017b), Naturally fractured hydrocarbon reservoir simulation by elastic fractures modeling. Petro Sci, 14, 286–301. https://doi.org/10.1007/s12182-017-0162-5

Tenzer, H., Park, C.H., Kolditz, O., McDermott, CI., (2010) Application of the geomechanical facies approach and comparison of exploration and evaluation methods used at Soultz-sous-Forêts (France) and Spa Urach (Germany) geothermal sites. Environ Earth Sci. 61(4) 853–880, https://doi.org/10.1007/s12665-009-0403-z

Vatandoust M, Farzipour Saein A, (2019) Fracture analysis of hydrocarbon reservoirs by static and dynamic well data, case study: The Aghajari oil field (the Zagros Fold-Thrust Belt). Develop in Struc Geol and Tect, 3, 1-16. https://doi.org/10.1016/B978-0-12-

815048-1.00001-9
Zhao, H., Ma, F., Liu, G., Feng, X., Guo, J., (2018) Analytical investigation of hydraulic fracture-induced seismicity and fault activation, Environ Earth Sci. 77:526, https://doi.org/10.1007/s12665-018-7708-8